AMPLITUDE-DEPENDENT PEAK AND RELAXATION SPECTRA OF WAVE ATTENUATION IN ROCK

E.I. MASHINSKII

Trofimuk Institute of Petroleum Geology and Geophysics, Siberian Branch of the RAS, prosp. Akad. Koptyuga 3, Novosibirsk 630090, Russia. MashinskiiEI@ipgg.nsc.ru

(Received December 28, 2010; revised version accepted April 27, 2012)

ABSTRACT

Mashinskii, E.I., 2012. Amplitude-dependent peak and relaxation spectra of wave attenuation in rock. *Journal of Seismic Exploration*, 21: 215-229.

The strain-amplitude and frequency dependencies of compressional- and shear-wave attenuation in siltstone have been experimentally studied. The measurements were performed using the reflection method on pulse frequency of 1 MHz, in the amplitude range $0.3 \leq \varepsilon \leq 2.0\ \mu$ strains under constant confining pressure of 10 MPa and ambient temperature. The nonlinear variation of quality factor (Q) depending on the strain-amplitude value ($\varepsilon_{min} \leftrightarrow \varepsilon_{max}$) is detected. The attenuation increment with increasing amplitude takes place only for a certain amplitude-value, further the decrease in attenuation occurs, and the amplitude-dependent peak $Q^{-1}(\varepsilon)$ appears. The relaxation spectrum of the P-wave attenuation $Q_P^{-1}(f)$ has the form of a monotonic curve with steepness which depends on the strain amplitude. The S-wave relaxation spectrum $Q_S^{-1}(f)$ characterizes the presence of a local attenuation peak that tends to vanish with the increase in strain amplitude. Anomalous attenuation behaviour can be explained by the joint action of viscoelastic and microplastic mechanisms. New knowledge can be used for diagnostics of rocks and materials, and the interpretation improvement of acoustical and seismic data.

KEY WORDS: inelasticity, stress-strain relation, hysteresis, nonlinearity, wave velocity, seismic attenuation, relaxation spectra.

0963-0651/12/$5.00

INTRODUCTION

Wave attenuation as a function of strain amplitude in different rocks has been dealt with in many studies (Mavko, 1979; Johnston and Toksöz, 1980; Stewart et al., 1983; Tutuncu et al., 1994; Johnson et al., 1996; Zinszner et al., 1997; Ostrovsky and Johnson, 2001). Most of the data were received by using a resonant method at frequencies of 1-20 KHz in the micro-strain range, and less through a pulse transmission technique at a frequency of about 1 MHz in the same amplitude range. Usually, it was accepted that amplitude increase causes wave velocity decrease and attenuation increase. This point of view prevailed for a long time, in spite of some conflicting data (Johnston and Toksöz, 1980; Zaitsev et al., 1999). These data show that in some cases amplitude increase causes wave velocity increase and attenuation decrease. This fundamentally alters our notion about wave propagation physics.

The assumption of dual behaviour of wave velocity caused by strain amplitude, was earlier made by Mashinsky (1994). This effect was explained by rock microplasticity. Firstly, microplasticity is a strain-dependent process. Secondly, solely the microplastic component of common deformation is able to increase and decrease in the course of the increasing stress. The theoretical studies (McCall and Guyer, 1994; Guyer et al., 1995) and the subsequent experiments (Mashinskii, 2005a), have shown the opportunity of decrease and increase in the elastic modulus in compliance with the curvature in the stress-strain relation, $\sigma(\varepsilon)$. The following observations have confirmed these results (Zaitsev et al., 1999; Mashinskii et al., 1999; Mashinskii, 2005b). Thus, the new quality in the behaviour of wave velocity was ascertained. However, changes in wave velocity values for the studied amplitude range are quite minor. In spite of this, a good reason for further search appeared. The experiments in the dry and water-saturated sandstones, showed that amplitude effects are more expressive for attenuation in comparison with wave velocity (Mashinskii, 2006, 2007). Wave attenuation is more sensitive to amplitude variation in water-saturated sandstone. The detected increase in the quality factor with increasing amplitude, extends notion about wave attenuation. Besides, other effects (for example, the amplitude-dependent variation of a relaxation spectrum of wave attenuation) was also detected.

The attenuation study in the amplitude-frequency area is of interest not only as an abstract science. New effects can be useful to improve the proposed diagnostic method in solving the applied problems of material science, acoustic logging, seismic prospecting and other applications (Dvorkin et al., 2003; Mavko and Dvorkin, 2005). This paper presents an experimental study of amplitude effect on wave attenuation, its relaxation spectra in siltstone under pressure. New scientific results extend notions about wave attenuation in rock.

EXPERIMENTAL PROCEDURE

The experiments were conducted on the samples at pulse frequency ~ 1MHz with the variable amplitude in the range (0.3 - 2.0) μ strain under a confining pressure of 10 MPa and constant ambient temperature. The studied rock is a coarse-grained siltstone taken from a depth of 3140 m. It contains fine-grained sandy fractions (30%), coarse-grained siltstone (up to 60%) and fine-grained siltstone (10%). Rock density is 2.48 g/cm^3, general porosity - 5%, and is in room-dry condition. The sample is a cylinder 2 cm long and 4 cm in diameter.

The experimental setup and a pulse transmission technique were used, described by Jones (1995) and Mashinskii (2005b, 2006, 2007). It is a three-layer model. The material of the first and third layers (buffer) is identical, and provides an identical reflection of waves on the borders. The rock sample is between these buffers. Excitation and reception of ultrasonic pulses (f ~ 1 MHz) are carried out by means of the piezoelectric elements rigidly fixed on the acoustic buffer. The transducer is polarized on a compressional- and shear-wave. Each transducer is combined as a source-receiver pair, providing the excitation and reception of P- or S-wave. In our measurements, the confining pressure of 10 MPa provides constant contact conditions on the borders of the buffer. Jones (1995) showed that measurements of Q, using this technique, can be made reliable for confining pressure higher than 5 MPa, since in this case, the degree of coupling between the rock sample and buffer-rods is sufficient for providing a stiff contact. Nevertheless, the reflection method for measuring the nonlinear properties of rocks, requires the buffer-rods to be in a welded contact with the rock sample. Therefore, we used the fluid couplant at all interfaces. Spencer (1981) also showed that a thin film (for example, the epoxy) for the bond (< 0.1 mm) has a negligible effect on the measurements. Interference from sidewall reflections due to the finite size of the samples, is to be neglected above 0.5 MHz (Jones, 1995). As is known from Winkler and Plona (1982), data below 400 KHz should be discarded because of uncorrected diffraction effects. The same advice is given by Stewart et al. (1983): the lower end of frequencies should be restricted to the frequencies above ~ 0.4 MHz to avoid problems associated with ultrasonic beam diffraction. Therefore, we used the frequency band $\Delta f_{\text{min-max}}$ = 0.52 - 1.41 MHz for the study of the relaxation spectra of attenuation. Frequency characteristics of attenuation are determined using the spectral ratio method and graphed for every strain-amplitude level.

The attenuation was calculated by using the relation (Winkler, 1983)

$$Q^{-1} = \alpha V/8.686\pi f = \alpha\lambda/8.686\pi \ . \tag{1}$$

where α is the attenuation coefficient in dB m^{-1}, V is the wave velocity in m s^{-1} and f is the frequency in Hz. The value of α is calculated using relations

$$\alpha(\omega) = (8.686/L)\ln[\{|R_{23}|A_{top}(f)/|R_{12}|A_{bot}(f)\}\{1 - R_{12}^2(f)\}] \quad , \qquad (2)$$

where L is twice the sample thickness (in m), $A_{top}(f)$ is the Fourier magnitude of the reflected pulse from the front of the sample (top buffer/rock interface), A_{bot} is the Fourier magnitude of the reflected pulse from the back face of the sample (bottom rock/buffer interface), $R_{12}(f)$ is the reflection coefficient between the coupling buffer and sample, and R_{23} is the reflection coefficient between sample and the backing buffer. In our case, the coupling and backing buffers are identical (beryllic bronze) therefore, $R_{12}(f) = -R_{23}(f)$. Coefficient R(f) is calculated from

$$R(f) = [\rho_r V_r(f) - \rho_b V_b(f)]/[\rho_r V_r(f) + \rho_b V_b(f)] \quad , \qquad (3)$$

where ρ_r and ρ_b are densities of rock and beryllic bronze buffer-rod (in kg/m^3), respectively, and $V_r(f)$ and $V_b(f)$ are their velocities (in m/s).

The amplitude effect study was conducted by variation of amplitude value over the closed cycle. The pulse amplitude discretely changes from minimum to maximum and back to minimum: $\varepsilon_{min} = \varepsilon_1 \rightarrow \cdots \vartheta_{max} = \vartheta_6 \rightarrow \vartheta_1$. They are $\vartheta_1 = 0.3$, $\vartheta_2 = 0.5$, $\vartheta_3 = 1.0$, $\vartheta_4 = 1.3$, $\vartheta_5 = 1.7$ and $\vartheta_6 = 2 \times 10^{-6}$ (microstrain). A cycle includes 11 amplitude magnitudes (six upward and five downward). Wave attenuation was measured at each amplitude level. Attenuation spectra were calculated for each frequency within the pulse bandwidth at six amplitude levels. For the pulse propagation, strain amplitude is estimated through the displacement amplitude u relative to the wavelength λ. Maximum strain magnitude can be calculated as: $\vartheta_M = \upsilon/V = 2\pi u/\lambda$, where υ is a particle velocity. Displacement u was estimated using the transmission coefficient of a piezoelectric transducer at the source voltage. Strain interval is approximately 10^{-7} - 10^{-6}. In this study, an accurate estimate is not obligatory, an order of magnitude is important here. Relative change in the attenuation with amplitude variation (under other constant conditions) is of great significance.

RESULTS

Fourier spectra

Time series of P- and S-wave for the incident pulse and second reflected pulse on six discretely upward and downward amplitudes are presented in Figs. 1 and 2. The time-intervals for the first and second pulse are indicated by the dotted lines. The second reflected pulse in the expanded scale is shown on the inset. There is a good reproducibility of results for the first and repeated measurements ($A_{1\text{-up}} = A_{1\text{-down}}$ etc.). Fourier spectra of P- and S-waves for the incident pulse and second reflected pulse were received on six discretely upward and downward amplitudes: $A^P_{inc}(f)$, $A^P_{bot}(f)$ and $A^S_{inc}(f)$, $A^S_{bot}(f)$. These spectra are shown in Figs. 3 and 4. The incident pulse is the first reflection from the front of the sample (top interface), and the second pulse, being the reflection from the back face of the sample (bottom interface), is a signal coming through the sample twice. Fourier spectra for upward and downward amplitudes coincide with each other well enough, and are therefore almost indistinguishable. A dominant frequency of the incident pulse is mainly f_{inc} = 0.945 MHz and 0.877 MHz for the P- and S-wave, respectively.

The spectrum form of $A^P_{bot}(f)$ is simple, however the upward and downward spectral curves slightly do not coincide. A dominant frequency of the second reflected pulse f^P_{bot} slightly increases with increasing amplitude. The spectrum form of the second reflected pulse $A^S_{bot}(f)$ is more complicated and has a strong complication in the low-frequency area. After the main maximum, there are maxima of higher order. Frequencies of subsequent spectral maxima are close to frequencies of the second and third oscillations harmonics. In this study, we are not allowed to overstep the limits of a narrow frequency range. It is necessary for the reliability of the results for the incident frequency.

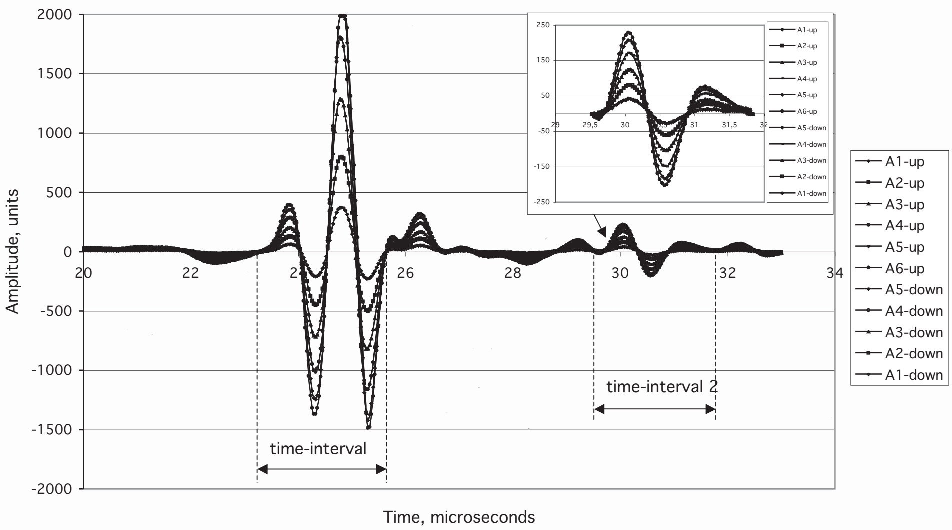

Fig. 1. Time series of the P-wave for the incident pulse and second reflected pulse on six discretely upward and downward amplitudes. The time-intervals for the first and second pulse are indicated by the dotted lines. The second pulse in expanded scale is shown on the inset.

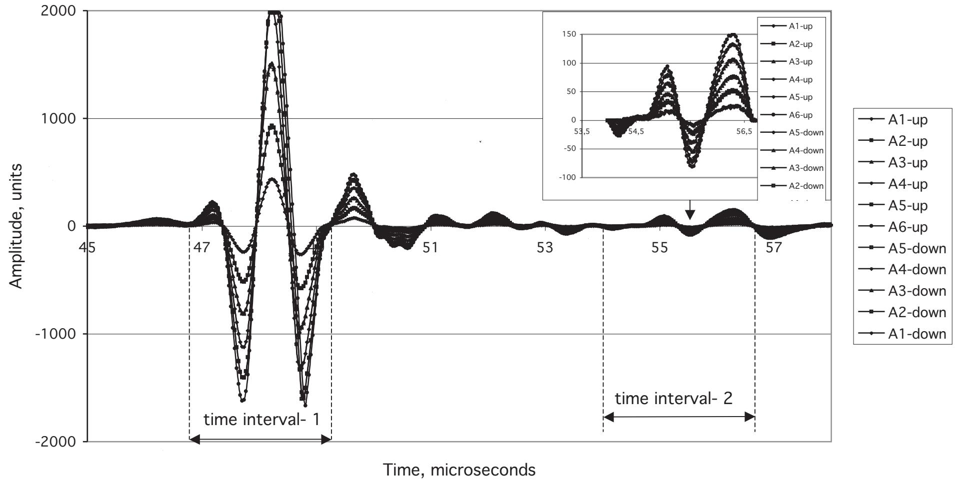

Fig. 2. Time series of the S-wave for the incident pulse and second reflected pulse on six discretely upward and downward amplitudes. The time-intervals for the first and second pulse are indicated by the dotted lines. The second pulse in expanded scale is shown on the inset.

Relaxation spectra of the wave attenuation

Dependencies of P- and S-wave attenuations in siltstone as a function of frequency for the six upward strain amplitudes under a confining pressure of 10 MPa, are presented in Figs. 5 and 6. Relaxation spectra of P-wave attenuation $Q_P^{-1}(f, |\vartheta_{1\text{-}6}|_{const})$ have a relatively simple form. Wave attenuation inversely depends on frequency. Nevertheless, relaxation spectra for different amplitudes all the same somewhat differ from each other in the shape of the curves and in their slope. An amplitude variation causes a slight shift of relaxation curve $Q_P^{-1}(f)$ in the X-Y coordinates. Increase in strain amplitude transforms the form of the relaxation curve. On the minimal amplitude, the dependence $Q_P^{-1}(f)$ is presented by the curve with variable slope, and on the maximum amplitude this dependence is close to linear. Besides, increase in strain amplitude causes increase in steepness of the frequency characteristic of attenuation, and at the same time its displacement towards the low frequencies.

Dependencies of shear wave attenuation as a function of frequency $Q_S^{-1}(f, |\vartheta_{1\text{-}6}|_{const})$ for the six upward strain amplitudes are presented in Fig. 6. The S-wave relaxation spectrum shows a monotonic decrease in attenuation with frequency in the predominant part of the spectrum with the local relaxation peak a)

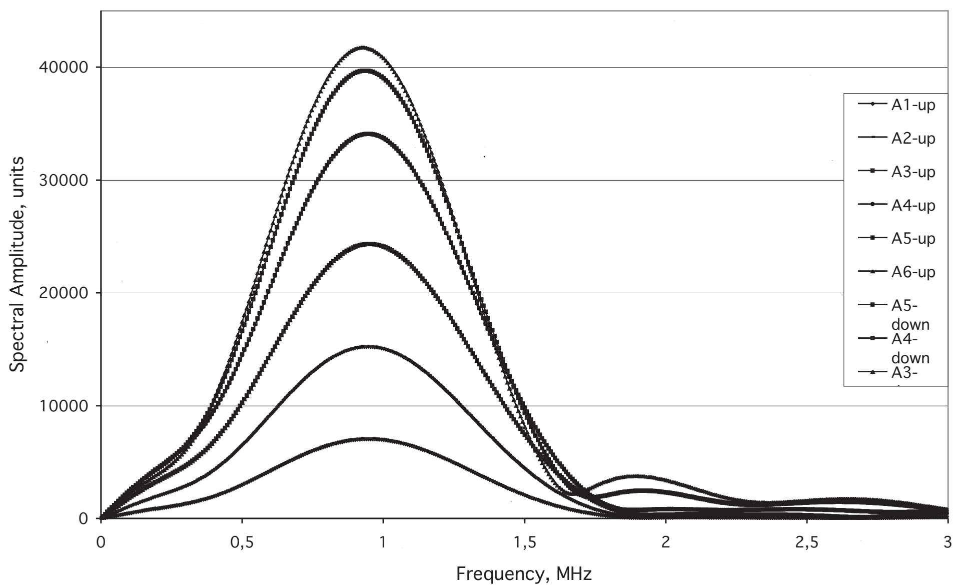

b)

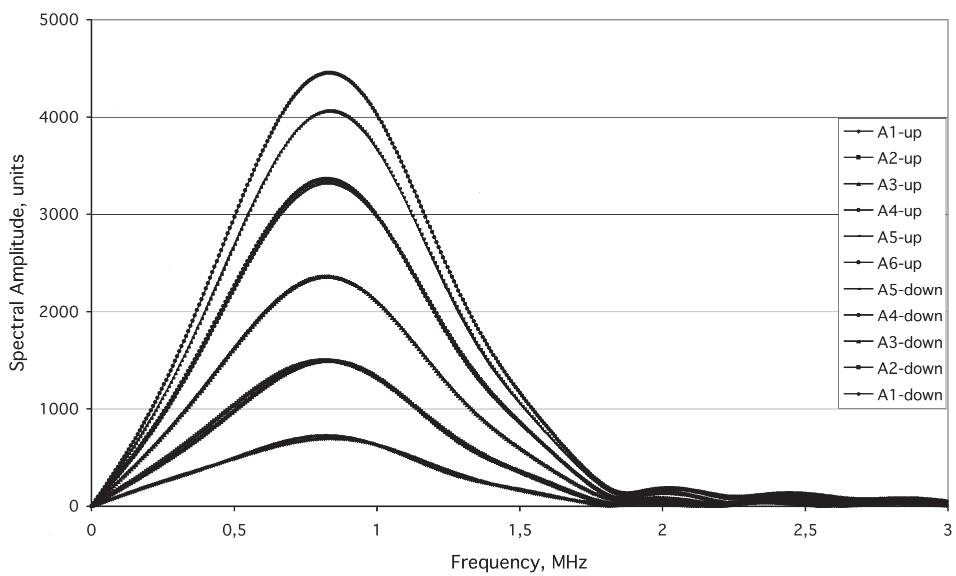

Fig. 3. P-wave Fourier spectra for the incident pulse (a) and the second reflected pulse (b) on six discretely upward and downward amplitudes.

a)

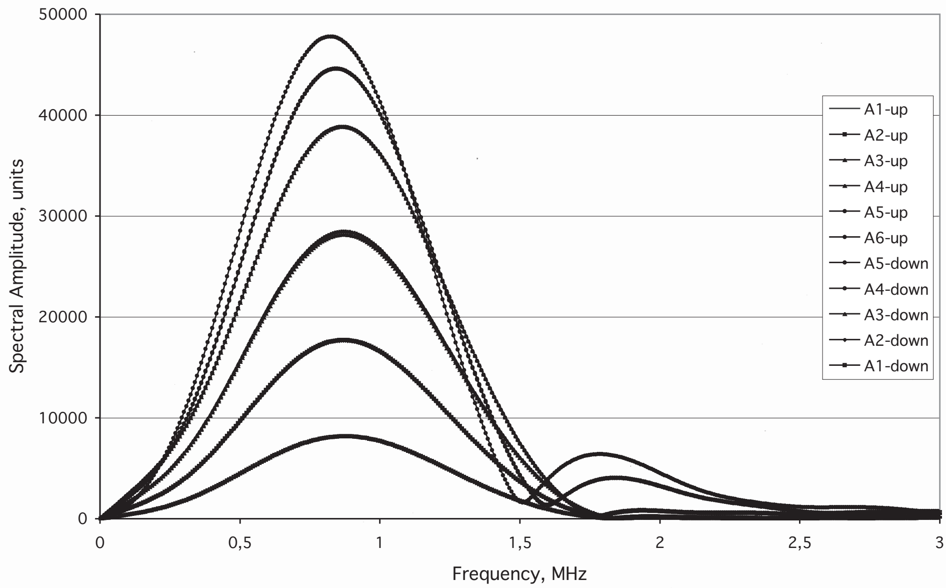

b)

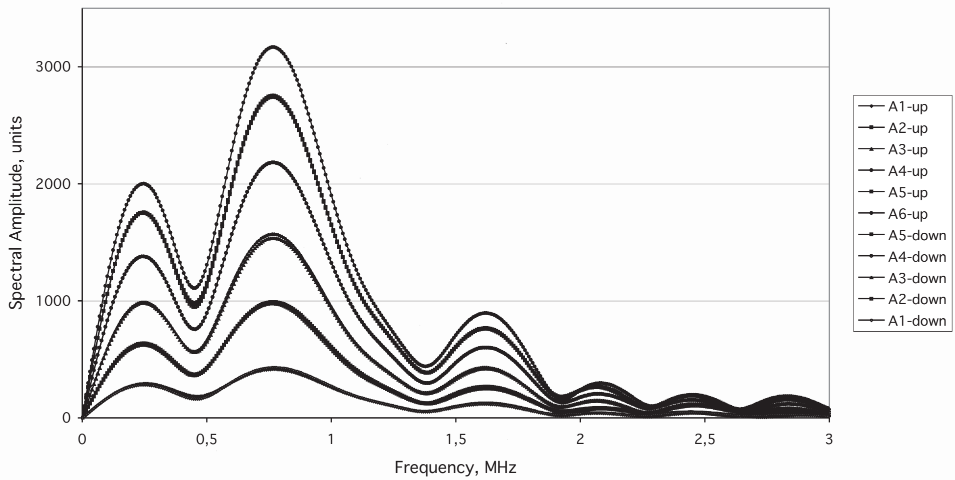

Fig. 4. S-wave Fourier spectra for the incident pulse (a) and the second reflected pulse (b) on six discretely upward and downward amplitudes.

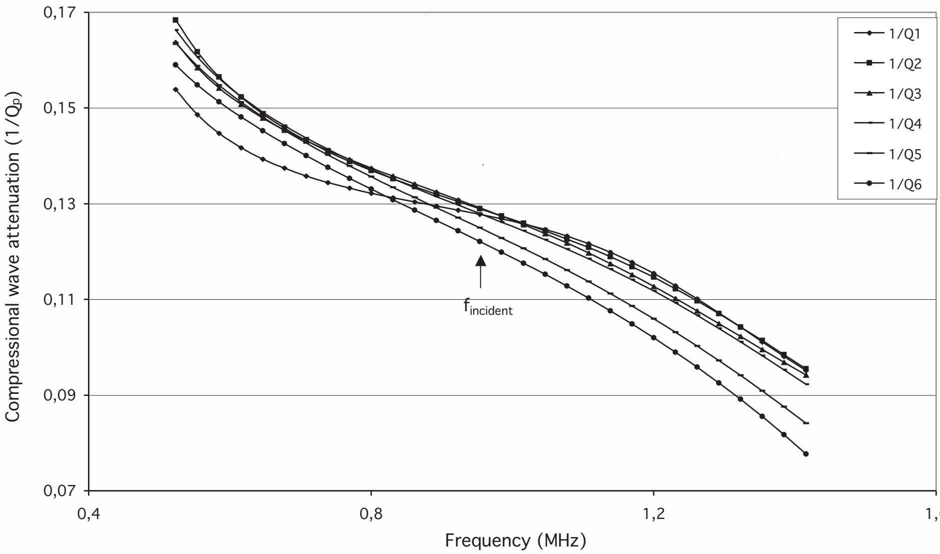

Fig. 5. Compressional wave attenuation in siltstone as a function of frequency for the six upward strain amplitudes. Confining pressure is equal to 10 MPa (further everywhere).

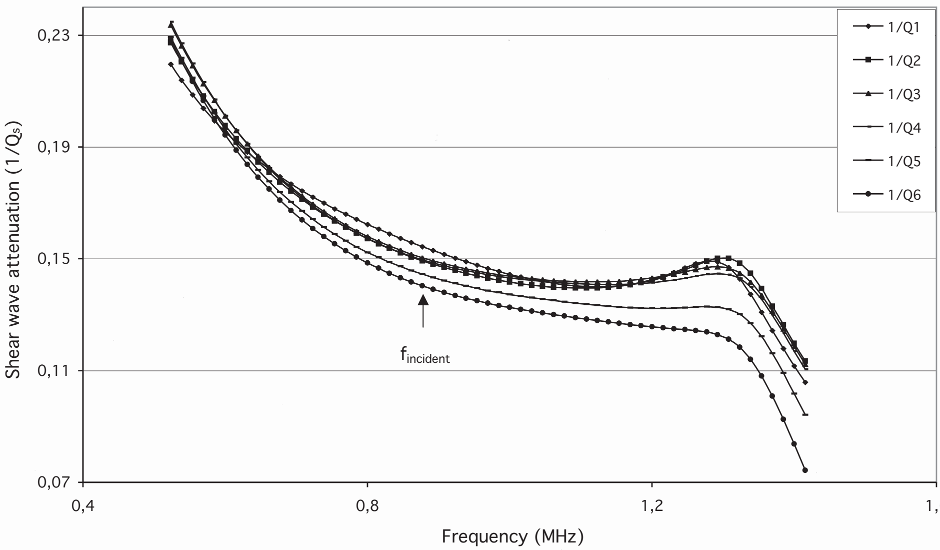

Fig. 6. Shear wave attenuation in siltstone as a function of frequency for the six upward strain amplitudes.

at its high-frequency end. The relaxation peak alters its own form in dependence on the strain amplitude. The increase in strain amplitude from minimum to maximum value leads to the gradual degradation and the subsequent disappearance of a local relaxation peak.

Influence of strain amplitude on wave attenuation

P- and S-wave attenuations as a function of the upward and downward amplitude $Q_P^{-1}(\vartheta)$ and $Q_S^{-1}(\vartheta)$ in siltstone for incident frequencies (0.945 MHz and 0.877 MHz, respectively) under pressure of 10 MPa, are presented in Fig. 7. Wave attenuation nonlinearly depends on strain amplitude. There is an amplitude-induced attenuation peak that denotes the inversion in the attenuation course caused by change in strain value. The attenuation value with the increase in strain amplitude first rises, and then decreases. The same effect takes place when strain amplitude decreases in the reverse sequence. The greatest change in the attenuation value caused by the strain-amplitude variation reaches about 7%. The S-wave shows monotonic decrease in attenuation with increasing amplitude, the presence of a small local peak nearby the 1.0 micro-strain.

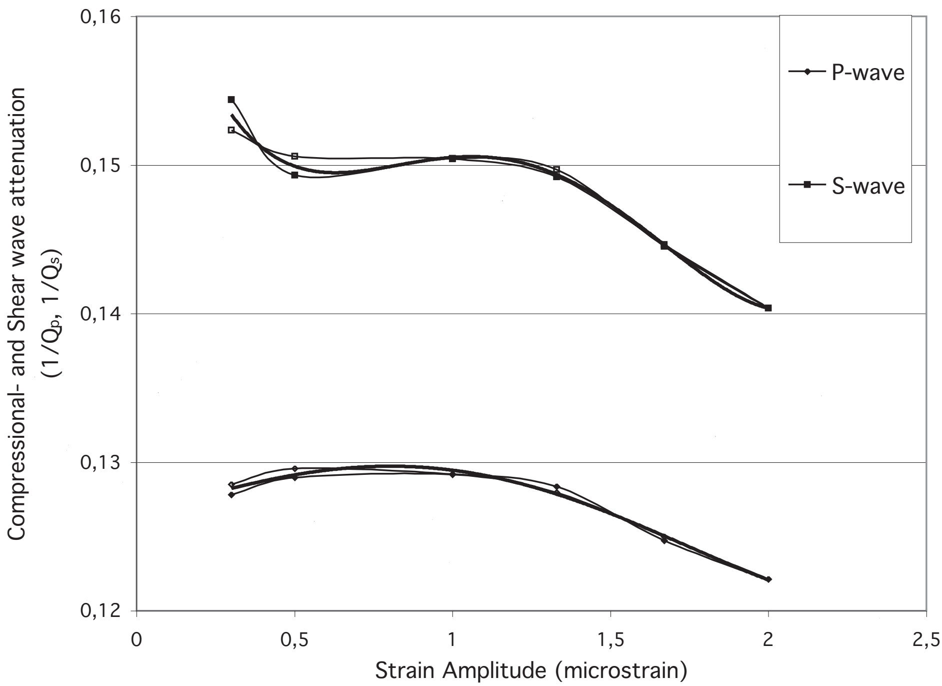

Fig. 7. Compressional and shear wave attenuation in siltstone as a function of the upward and downward strain amplitude ($\varepsilon_1 \rightarrow \varepsilon_6 \rightarrow \varepsilon_1$) for the incident frequency. A polynomial approximation is made. The solid marker is the upward amplitude course, and the open marker is the downward amplitude course.

P- and S-wave attenuations in siltstone as a function of upward strain amplitude for different frequency components are presented in Fig. 8. P-wave attenuation curves for the incident frequency and all frequencies situated below (low-frequency region) are nearly similar. These amplitude dependencies have a peak form. The attenuation peak on the frequencies above the incident frequency, in the high-frequency (unrelaxed) range, gradually vanishes with the increase in frequency, and the curve acquires the monotonic character with variable steepness. The S-wave local peak takes place for all frequency components of the relaxation spectrum. Curves of the amplitude dependence of the S-wave attenuation for all frequency components are practically parallel to each other, and therefore they are practically identical. The span between these curves is uneven and decreases with the increase in frequency. Change in span occurs because the slope (steepness) of the frequency response of S-wave attenuation changes.

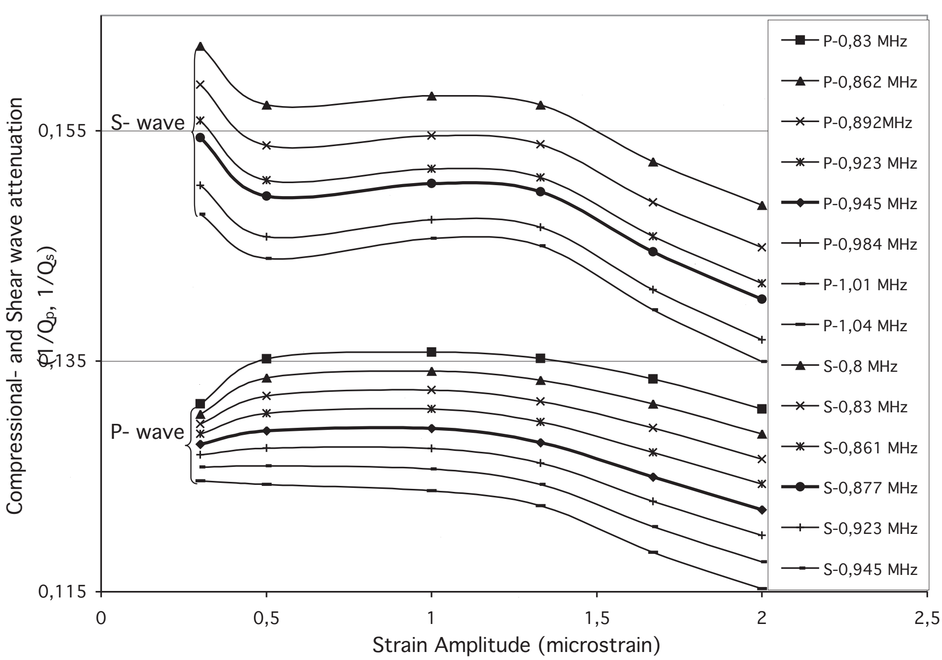

Fig. 8. Compressional and shear wave attenuation in siltstone as a function of the upward strain amplitude for the different frequency components. A polynomial approximation is made.

DISCUSSION

The attenuation study in siltstone confirms data for sandstone and quartz (Mashinskii, 2006, 2007, 2008) and demonstrates a new effect. The amplitude-dependent attenuation peak for rock is the unusual inelasticity manifestation. Material science confirms and explains the amplitude-dependent attenuation peak in solid states. For example, the bygone theory of Rogers (Rogers, 1962) predicts the attenuation maximum $Q^{-1}(\vartheta_0)$, where ϑ_0 is the strain amplitude. This is the modified dislocation theory of athermic tearing off from admixture of the different dislocations type. Amplitude-dependent peak of attenuation was detected in metal alloy and described with the help of a phenomenological model in experimental-theoretic work (Arzhavitin, 2004). In this model, the internal friction mechanism is considered as a hybrid relaxation-hysteresis process. The contour of a hysteresis loop $\sigma(\vartheta)$ is given by equation

$$\sigma = E\vartheta \pm \eta(|e| + |\vartheta|)^n|\dot{\vartheta}|^m \ , \tag{4}$$

where $|e|$, $|\vartheta|$, $|\dot{\vartheta}|$ are absolute magnitudes of preliminary deformation, current microplastic deformation independent of time, and the microplastic-deformation rate, respectively (e indicates that the appearance of microplastic deformation occurs only after the stress exceeds some critical magnitude); E is the Young's modulus, η is the effective viscosity of material, n is an index of strain strengthening, m is an index of rate strengthening. Indices show that microplasticity is sensitive to a degree of deformation (n) and deformation rate (m). Amplitude dependence of internal friction is given by

$$Q^{-1} = (1/\pi E\varepsilon_0^2) \oint \sigma d\varepsilon = (4/\pi E\varepsilon_0^2) \cdot \int_0 \eta(e + \varepsilon)^n \dot{\varepsilon}^m d\varepsilon$$

$$= \{4\eta[(e + \varepsilon_0)^{n+1} - e^{n+1}]\dot{\varepsilon}^m\}/\pi(n + 1)E\varepsilon_0^2 \ , \tag{5}$$

where $\Delta W = \oint \sigma d\varepsilon$ is the "square" of the hysteresis loop in the $\sigma - \varepsilon$ coordinates, ε_0 is the strain amplitude. The relationship (5) describes an internal friction with the hysteresis and relaxation processes simultaneously since Q^{-1} depends on ε_0 and $\dot{\varepsilon}$. The expression (5) becomes simpler if we consider that microplasticity manifestations take place on very small deformations (e = 0):

$$Q^{-1} = 4\eta\varepsilon_0^n\dot{\varepsilon}^m/\pi(n + 1)\varepsilon_0 E \ . \tag{6}$$

If the strain strengthening is absent (n = 0), then from (6) we receive

$$Q^{-1} = 4\eta\dot{\varepsilon}^m/\pi E\varepsilon_0 \ . \tag{7}$$

As can be seen from expression (6), the behaviour of internal friction with strain amplitude depends on the n magnitude. The increase in the internal friction with increasing amplitude takes place in that case when $n > 1$. The internal friction decreases with increasing strain amplitude when $n < 1$ or equals to zero (7). Transition from the upward to downward strain-amplitude dependence is accompanied by the jump in the n value. Thus, wave attenuation obeys the following rule

$$Q^{-1}_{P,S} \propto k\varepsilon_0^{\pm\tilde{n}} \quad , \qquad (8)$$

where k is the dimensionless coefficient. The exponent ñ determines the steepness (the slope of the line) of attenuation variation with amplitude.

The experiment shows that wave attenuation in siltstone behaves in the same way. In the restricted amplitude range, attenuation first increases and then decreases. Such behaviour of wave attenuation in the dependence on amplitude is altogether typical for rock microplasticity. The point is that microplasticity contribution in the deformation process can both increase and decrease in dependence on wave intensity, and thereby influences the wave characteristics (Mashinskii, 2005a). It is necessary to mention that viscous elasticity does not allow such behaviour. In spite of the external similarity of microplastic effects in rocks and metals, there are manifestations of microplasticity in rock that are indistinctive for metals. Some of the rocks show so-called threshold effect. During deformation on reaching the threshold stress, the sign change in the microplasticity behaviour occurs: increase ceases, decrease appears and vice versa. Such alternation is possible due to the more complicated microstructure of rock in comparison with metals. Therefore, hybrid relaxation-hysteresis mechanism of attenuation in rock in modified form is quite possible. It is necessary to note also that the author of the work (Arzhavitin, 2004) does not consider the influence on attenuation of the strain rate $\dot{\varepsilon}$. I suppose that for rock this parameter is of great importance. For example, the $\dot{\varepsilon}$ can also both increase and decrease with increasing strain. Behaviour of rock viscosity in dependence on applied stress also needs a special study.

Comparison of previous data (Mashinskii, 2006, 2007, 2008) with the last result, shows that the wave attenuation in sandstones and quartz crystals as a rule decreases monotonically with increasing strain amplitude. Attenuation peak (i.e., the presence of increase and decrease in attenuation) in the same amplitude range is detected in an explicit form, for the time being only in siltstone. It is an apparently peculiar feature of this rock. The amplitude dependence of wave attenuation in the form of a peak in the small-strain range is a new fact that requires subsequent study.

The amplitude exerts influence on the relaxation spectrum form. Frequency dependencies of P-wave attenuation in siltstone do not have a relaxation peak. The amplitude influence consists in the change of the curve slope and its form. Frequency response of S-wave attenuation contains a local peak, dependent of amplitude. It is necessary to note that the fact of relaxation peak by itself, in the same frequency domain in sandstone, has been known a long time (Tutuncu et al., 1994). The frequency shift of a peak in sandstone is caused by variation in clay content. Beside in sandstone, the relaxation peak in the same frequency band is detected also in Lucite (Prasad and Manghnani, 1997). The effect of degradation and even disappearance of the relaxation peak under the influence of strain amplitude, presents a new knowledge presented in this study.

CONCLUSION

During the study of wave attenuation in one siltstone, an unusual effect was detected. The principal result is the detection of an amplitude-dependent attenuation peak. An attenuation peak known in metals and alloys, is connected with microplasticity. I suppose the amplitude-dependent peak of wave attenuation in rock can also be caused by the same effect, as there are reasons for it. Unusual manifestations of microplasticity at meso- and micro-level are detected in many rocks during quasi-static deformation (Mashinskii, 2005a). Microplastic inelasticity can most probably be a reason for the amplitude-dependent behaviour of wave velocity and attenuation during propagation of seismic and acoustic waves. Research, for example by Faul et al. (2004) gives hope that thin grain boundaries (1 nm wide) can produce inelastic attenuation peaks, jointly with effects of microplasticity existent at nano-level. These problems affect the little-known inelastic processes of small-amplitude wave propagation. I hope that new knowledge of nonlinear-inelastic processes during wave propagation will help to discover new diagnostic indications, allowing to increase the efficiency of seismic and acoustical methods.

ACKNOWLEDGEMENTS

The author thanks Dr. I.R. Obolentseva for the interesting discussion of experimental results and the anonymous referee for the useful comments that has improved this work considerably.

REFERENCES

Arzhavitin, V.M. 2004. Amplitude dependence of the internal friction in a Pb-62% Sn Alloy. Technic.l Phys., 49: 707-710.

Dvorkin, J., Walls, J., Taner, T., Derzhi, N. and Mavko, G., 2003. Attenuation at patchy saturation: a model. Extended Abstr., 65th EAGE Conf, Stavanger.

Faul, U.H., Fitz, G.J.D. and Jackson, I., 2004. Shear wave attenuation and dispersion in melt-bearing olivine polycrystals: 2. Microstructural interpretation and seismological implications. J. Geophys. Res., 109: B06202.

Guyer, R.A., McCall, K.R. and Boitnott, G.N., 1995. Hysteresis, discrete memory and nonlinear wave propagation in rock: a new paradigm. Phys. Rev. Lett., 74: 3491-3494.

Johnson, P.A., Zinszner, B. and Rasolofosoan, P.N.J., 1996. Resonance and elastic nonlinear phenomena in rock. J. Geophys. Res., 101: 11553-11564.

Johnston, D.H. and Toksöz, M.N., 1980. Thermal cracking and amplitude dependent attenuation. J. Geophys. Res., Vol. 85: 937-942.

Jones, S.M., 1995. Velocity and quality factors of sedimentary rocks at low and high effective pressures. Geophys. J. Int., 123: 774-780.

Mashinskii, E.I., Koksharov, V.Z. and Nefedkin, Yu.A., 1999. Amplitude-dependent effects in the range of small seismic strains. Geol. Geofiz, 40: 611-618.

Mashinskii, E.I., 2005a. Non-linear stress-strain relation in sedimentary rocks and its effect on seismic wave velocity. Geophysics, 41: 3-17.

Mashinskii, E.I., 2005b. Experimental study of the amplitude effect on wave velocity and attenuation in consolidated rocks under confining pressure. J. Geophys. Engin., 2: 199-212.

Mashinskii, E.I., 2006. Nonlinear amplitude-frequency characteristics of attenuation in rock under pressure. J. Geophys. Engin., 3: 291-306.

Mashinskii, E.I., 2007. Effect of strain amplitude on the relaxation spectra of attenuation in dry and saturated sandstone under pressure. J. Geophys. Engin., 4: 194-203.

Mashinskii, E.I., 2008. Amplitude-frequency dependencies of wave attenuation in single-crystal quartz: experimental study. J. Geophys. Res., 113: B11304.

Mashinsky, E.I., 1994. Quasi-micro-plasticity processes and nonlinear seismicity. Phys. Solid Earth, 30: 97-102.

Mavko, G.M., 1979. Friction attenuation: an inherent amplitude dependence. J. Geophys. Res., 84: 4769-4775.

Mavko, G. and Dvorkin, J., 2005. P-wave attenuation in reservoir and non-reservoir rock. Extended Abstr., 67th EAGE Conf., Madrid.

McCall, K.R. and Guyer, R.A., 1994. Equation of state and wave propagation in hysteretic nonlinear elastic materials. J. Geophys. Res., 99: 23887-23897.

Ostrovsky, L.A. and Johnson, P.A., 2001. Dynamic nonlinear elasticity in geomaterials. Rivis. Nuovo Cimento, 24: 1-37.

Prasad, M. and Manghnani, M.H., 1997. Effect of pore and differential pressure on compressional wave velocity and quality factor in Berea and Michigan sandstones. Geophysics, 62: 1163-1176.

Rogers, D.H., 1962. An extension of a theory of mechanical damping due to dislocation. J. Appl. Phys., 33: 781-792.

Spencer, J.W., 1981. Stress relaxation at low frequencies in fluid-saturated rocks: attenuation and modulus dispersion. J. Geophys. Res., 86: 1803-1812.

Stewart, R.R., Toksöz, M.N. and Timur, A., 1983. Strain dependent attenuation: observations and a proposed mechanism. J. Geophys. Res., 88: 546-554.

Tutuncu, A.N., Podio, A.L. and Sharma, M.M., 1994. An experimental investigation of factors influencing compressional- and shear-wave velocities and attenuations in tight gas sandstones. Geophysics, 59: 77-86.

Winkler, K.W. and Plona, T.J., 1982. Technique for measuring ultrasonic velocity and attenuation spectra in rocks under pressure, J. Geophys. Res., 87: 10776-10780.

Winkler, K.W., 1983. Frequency dependent ultrasonic properties of high-porosity sandstones. J. Geophys. Res., 88: 9493-9499.

Zaitsev, V.Yu., Nazarov, V.E. and Talanov, V.I., 1999. Experimental Study of the Self-Action of Seismoacoustic Waves. Acoust. Physics, 45: 720-726.

Zinszner, B., Johnson, P.A. and Rasolofosoan, P.N.J., 1997. Influence of change in physical state on elastic nonlinear response in rock: Significance of effective pressure and water saturation. J. Geophys. Res., B102: 8105-8120.